

## Research Article

# Identification of Mine Water Source Based on AHP-Entropy and Set Pair Analysis

Xianming Zhao , Zhimin Xu , and Yajun Sun 

School of Resources and Geosciences, China University of Mining and Technology, Xuzhou 221116, China

Correspondence should be addressed to Zhimin Xu; xuzhimin@cumt.edu.cn

Received 2 March 2022; Accepted 23 March 2022; Published 27 April 2022

Academic Editor: Constantinos Loupasakis

Copyright © 2022 Xianming Zhao et al. This is an open access article distributed under the Creative Commons Attribution License, which permits unrestricted use, distribution, and reproduction in any medium, provided the original work is properly cited.

After a water inrush disaster occurs in the mine production process, it is urgent to identify the source of water inrush and formulate corresponding countermeasures in the complex hydrogeological condition of coal mines. Therefore, accurate identification of mine groundwater source is one of the keys to prevent mine water disasters. According to the difference between the hydrochemical compositions of three aquifers in Chengjiao coal mine, six primary ions ( $Na^+ + K^+$ ,  $Ca^{2+}$ ,  $Mg^{2+}$ ,  $SO_4^{2-}$ ,  $Cl^-$  and  $HCO_3^-$ ) were selected as the indexes for groundwater source identification. On this basis, a mathematical model for groundwater source identification was established by combining the analytic hierarchy process- (AHP-) entropy weight method and the set pair analysis (SPA) theory. Next, this model was used to identify the sources of 10 sets of water samples from the mine, and then, the identification results were compared with the results of conventional models established using Fisher discriminant analysis (FDA) and Bayes discriminant analysis (BDA) methods. The results show that the SPA-based model performs better in identifying the groundwater sources. Furthermore, the model was used to identify the source of water inflow in the No. 21304 panel. The analysis on identification results reveals that the area close to the  $F_{20}$  normal fault tends to receive water supply from the Ordovician limestone aquifer and the Taiyuan Formation limestone aquifer, so it should be regarded as a key area for water inrush prevention and control.

## 1. Introduction

China is the largest coal producer and consumer in the world. The coal mass production was 3.84 billion tons in 2020, and it kept increasing at the rate of about 0.9% according to the Energy Production Report (2020) released by the National Bureau of Statistics of China. At present, coal plays an important role in China's economic development, accounting for 62% and 68.5% of China's energy structure and energy consumption, respectively. However, water disasters happened frequently in the mining process due to complex hydrogeological conditions of Chinese coal mines [1]. Groundwater may inrush into the mine roadway suddenly when faults, mined-out space, and karst collapse columns are affected and broken during mining activities. The mine water inrush is ferocious, often engulfing the roadway in an instant and resulting in considerable casualties and economic losses. A total amount of 779 water disasters happened in China, which resulted in

enormous casualties (3,831 deaths) and economic losses in the period 2000-2020 [2]. After a water inrush disaster occurs in mine production processing, it is urgent to identify the source of water inrush and formulate the corresponding control measures, and varied control measures should be made out for the different aquifer conditions based on water richness. For aquifers with less water, the water inrush hazards could generally be eliminated through temporary water bin construction in low-lying areas or enough water pump installation. However, for those with rich water aquifers, water inrush hazards were often controlled by grouting into aquifer's fissures and transforming it into aquiclude or retaining water-resisting coal pillars [3]. In a word, rapid and accurate groundwater source identification is essential for reasonable selection and optimization of water control measures [4-6].

It is an essential step to reasonably determine the weight of each identification index in groundwater source identification [7-9]. While the above methods we mentioned

promoted the identification accuracy, they still have some restrictions to comply with, for instance, the certain random weight assignment and fuzzy indexes were generally generated based on artificial experiences. Researches that were conducted by using this method could neither overcome the complicacy and fuzziness of the multiaquifer system nor fully represent the hydrochemical characteristics of the aquifers and increase the inaccuracy of the identification results. In order to solve this problem, this paper combined the AHP- (analytic hierarchy process-) entropy weight method and the SPA (set pair analysis) theory to establish a new groundwater source identification model. To be specific, the objective weight was calculated based on information entropy, while the subjective weight was calculated by the means of AHP. Then, the two weights were combined for calculating a comprehensive weight for each identification index. This weighting method not only reflects the knowledge and experiences of experts but also avoids the subjectivity of traditional experience-based methods [10–12]. It is successful to ensure the scientific nature and comprehensiveness of the weight of mine water source identification indexes.

The SPA theory, proposed by a Chinese scholar named Keqin Zhao in 1989, is a systematic analysis method for uncertain issues [13, 14]. It has been applied in various fields, such as building sustainable performance [15], disease hazard [16], efficacy of medicine, tourism resources [17], urban ecosystem [18], information technology [19], water environment [20, 21], and water resource system [22]. It focuses on the relationship between the accurate and inaccurate features of two related data sets and establishes the relationship between them in a mathematical form, and this form could be identified by identity-discrepant-contrary coefficients. There generally exist several aquifers that are capable of supplying inrush water to be identified. These aquifers could hardly be identified accurately through a single index due to their significantly varied hydrochemical characteristics and obsolete boundaries. This problem could be effectively solved by SPA. A SPA theoretical mathematical model was established to promote the accuracy of groundwater source identification based on the characteristic values of water samples from potential aquifers.

In this work, a mathematical model for mine water source identification was proposed based on the analytic hierarchy process- (AHP-) entropy weight method and the set pair analysis (SPA) theory. In addition, water samples extracted from different aquifers in Chengjiao coal mine were screened for excluding abnormal data by the means of the Piper trilinear diagram and the cluster analysis. Finally, characteristic values of water samples from potential aquifers were determined. This practical study not only provides a positive reference for identifying groundwater sources but also lays an important foundation for optimizing water disaster prevention and control schemes.

## 2. Materials and Methods

*2.1. The AHP-Entropy Weight Method.* The AHP-entropy weight method, a weighting method that combines the

objective weight with the subjective weight, varied with the conditions of the object to be evaluated. It comprehensively considers subjective and objective situations to ensure the rationality of the assignment of index weight. The objective weight of each index was calculated by using the entropy weight method. According to the definition of entropy, the entropy of the  $j$ th ( $j = 1, 2, \dots, n$ ) index could be expressed as

$$E_j = -\frac{\sum_{i=1}^m f_{ij} \ln f_{ij}}{\ln m}, \quad j = 1, 2, \dots, n, \quad (1)$$

where  $m$  is the total number of samples;  $n$  is the total number of indexes;  $f_{ij} = v_{ij}/\sum_{i=1}^m v_{ij}$ ;  $v_{ij}$  is the quantity value of each index of each water source; and if  $f_{ij} = 1$ , then  $f_{ij} \ln f_{ij} = 1$ . The entropy weight value of the  $j$ th index could be calculated by

$$\delta_j = \frac{1 - E_j}{\sum_{j=1}^n (1 - E_j)}, \quad j = 1, 2, \dots, n. \quad (2)$$

The subjective weight of each index was obtained by means of AHP. First, the importance of indexes was compared to establish a judgment matrix. Meanwhile, the characteristic equation was solved:

$$AR = \lambda_{\max} R, \quad (3)$$

where  $\lambda_{\max}$  is the maximum eigenvalue of the judgment matrix  $A$ ;  $R = (r_1, r_2, \dots, r_n)$  is the eigenvector of  $\lambda_{\max}$ . Then, the subjective weight vector of the  $j$ th index could be obtained after normalizing the eigenvector  $R$ :

$$\theta_j = \left( \frac{r_1}{\sum_{j=1}^n r_j}, \frac{r_2}{\sum_{j=1}^n r_j}, \dots, \frac{r_n}{\sum_{j=1}^n r_j} \right). \quad (4)$$

Finally, the comprehensive weight of the  $j$ th index could be determined by combining the objective weight with the subjective weight:

$$\omega_j = \frac{\delta_j \theta_j}{\sum_{j=1}^n \delta_j \theta_j}, \quad j = 1, 2, \dots, n. \quad (5)$$

*2.2. The SPA Theory.* SPA is a systematic analysis method to deal with the problem of uncertainty in nature. Its core idea is to use dialectical analysis (identity, discrepancy, and contradistinction) for describing the uncertainty of things, which means to describe the uncertainty with a certain degree of connection [23]. In the process of mine groundwater source identification, it is assumed that the degree of connection between the set  $U$  and the set  $V$  is expressed by  $\mu$ , and the two sets constitute the set pair  $H$ , and  $H = (U, V)$ . The degree of connection  $\mu$  could be expressed by a mathematical expression:

$$\mu = a + bi + cj. \quad (6)$$

Equation (6), referred to as the ternary degree of connection, is the basic formula of SPA.  $a$ ,  $b$ , and  $c$  in the equation, commonly known as three components of the degree of connection, are the identity coefficients, the discrepant coefficient, and the contrary coefficient, respectively. In order to adapt to the complexity, ambiguity, and comprehensiveness of mine groundwater source identification, Equation (6) could be extended into

$$\mu = a + (b_1 + b_2)i + (c_1 + c_2)j = a + b_1i^+ + b_2i^- + c_1j^+ + c_2j^-, \quad (7)$$

where  $b_1$  and  $b_2$  are the coefficients of the water source type's left and right adjacent intervals;  $c_1$  and  $c_2$  are the coefficients of the water source type's secondary left and right adjacent intervals;  $a + b_1 + b_2 + c_1 + c_2 = 1$ ,  $i^- \in [-1, 0]$ ,  $i^+ \in [0, 1]$ ,  $j^+ = \{0, 1\}$ , and  $j^- = -1$ . The intervals of mine groundwater source identification are interpreted in Figure 1. The whole identification interval was equally divided into three parts, namely, the water source type's membership interval (1/3 in total), the adjacent intervals (1/3 in total), and the secondary adjacent intervals (1/3 in total). That is, the left adjacent interval, secondary left adjacent interval, right adjacent interval, and secondary right adjacent interval account for 1/6 of the whole identification interval, respectively.

$$S_4 - S_1 = 2(S_3 - S_2), \quad (8)$$

where  $S_2$  and  $S_3$  are the lower and upper limits of a certain index in the water source type's membership interval, respectively;  $S_1$  and  $S_4$  are the lower and upper limits of this index in the water source type's adjacent intervals, respectively.

Assuming that the water sample to be evaluated is  $X = [x_1, x_2, \dots, x_n]$ , then the calculation formulas for the connection degree components of  $X$ 's  $p$ th index  $x_p$  ( $p = 1, 2, \dots, n$ ) are displayed as

$$\mu = a + b_1i^+ + b_2i^- + c_1j^+ + c_2j^- = \begin{cases} \frac{S_3 - S_2}{S_3 - x_p} + \frac{S_2 - S_1}{S_3 - x_p}i^- + \frac{S_1 - x_p}{S_3 - x_p}j^- & x_p < S_1, \\ \frac{S_3 - S_2}{S_3 - x_p} + \frac{S_2 - x_p}{S_3 - x_p}i^- & S_1 \leq x_p < S_2, \\ 1 & S_2 \leq x_p < S_3, \\ \frac{S_3 - S_2}{x_p - S_2} + \frac{x_p - S_3}{x_p - S_2}i^+ & S_3 \leq x_p < S_4, \\ \frac{S_3 - S_2}{x_p - S_2} + \frac{S_4 - S_3}{x_p - S_2}i^+ + \frac{x_p - S_4}{x_p - S_2}j^+ & S_4 \leq x_p. \end{cases} \quad (9)$$

With the aid of the components of connection degree, the set pair trend between  $X$  and a certain water source type's identification interval could be calculated by

$$t = \frac{\sum_{p=1}^n \omega_p a}{\sum_{p=1}^n \omega_p (b_1 + b_2 + c_1 + c_2)}, \quad (10)$$

where  $\omega_p$  is the comprehensive weight of  $X$ 's  $p$ th ( $p = 1, 2, \dots, n$ ) index;  $t$  is the set pair trend. When  $t > 1$ ,  $X$  and the water source type's identification interval share the same trend in the dialectical relationship; and the larger the value of  $t$ , the stronger the trend. Thus,  $X$ 's water source type could be determined by Equation (10).

### 3. The Geological Setting

**3.1. Study Area.** Chengjiao coal mine is located in Yongcheng City, Henan Province, China (Figure 2). Overall, the mine's high altitude is in the north and the west and lower in the south and the east. The surface water system is poorly developed, and vertical infiltration of atmospheric precipitation is the main source of groundwater supply here. The main mining coal seam, i.e., the II<sub>2</sub> coal seam, is located in the Lower Permian Shanxi Formation. The main sources of groundwater are the Shanxi Formation sandstone aquifer, the Taiyuan Formation limestone aquifer (in the upper section), and the Ordovician limestone aquifer. Besides, a fully developed fault destroys the continuity of the aquiclude and facilitates hydraulic connections between aquifers, which immensely impedes water control in the mine.

**3.2. Major Hydrological Problem.** The No. 21304 panel, whose plane position is exhibited in Figure 2, is the first mining face in the south wing of the mine. The  $F_{20}$  fault lies outside the panel, and its profile section is shown in Figure 2. Since the fault throw is greater than 400 m, the top surface of Ordovician limestone in the fault footwall rises to an elevation of about -510 m which is far higher than the current coal seam elevation (-880 m) of the panel. If the fault is able to conduct aquifers' water, Ordovician limestone water near the opposite and foot of the fault is likely to flow into the panel through the fractures and cracks and pose considerable threats to mining operation safety. Hence, the groundwater source is necessary to be identified accurately in the panel, so that the corresponding water control measures could be formulated to ensure safe mining in this region.

### 4. Results and Discussion

**4.1. Establishment of an Identification Model.** To identify the groundwater source accurately in the No. 21304 panel, the AHP-entropy weight method and the SPA theory were combined to establish an identification model through the NumPy library of Python software. Figure 3 shows the workflow of the identification model.

The specific steps are as follows:

Step 1. Sampling.

Hydrochemical characteristics, especially main ion contents ( $Na^+ + K^+$ ,  $Ca^{2+}$ ,  $Mg^{2+}$ ,  $SO_4^{2-}$ ,  $Cl^-$ , and  $HCO_3^-$ ), are the basis of establishing a groundwater source identification model. In this study, a total of 47 water samples (1 to 47 in

	$S_1$	$S_2$	$S_3$	$S_4$
Secondary leftadjacent interval	Left adjacent interval	Water source type's membership interval	Right adjacent interval	Secondary right adjacent interval
1/6	1/6	1/3	1/6	1/6

FIGURE 1: Zoning interpretation of extended set pair.

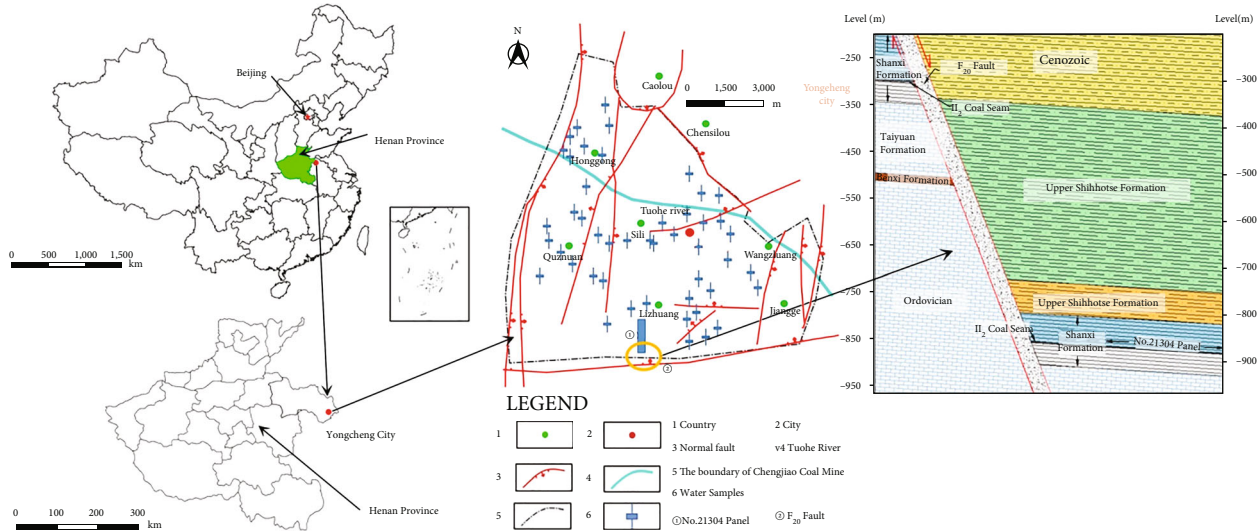


FIGURE 2: Location of Chengjiao coal mine and histogram of the No. 21304 panel.

Supplemental File) were extracted from different sampling sites of the three aquifers to establish the model.

#### Step 2. Exclusion of abnormal data.

The water samples were screened by means of the Piper trilinear diagram and the cluster analysis to exclude exceptional samples. In this way, the remaining ones could faithfully reflect the characteristic values of corresponding aquifers.

The Piper trilinear diagram, first proposed by Piper in 1944 [24], indicates the contents of six primary ions  $Na^+ + K^+$ ,  $Ca^{2+}$ ,  $Mg^{2+}$ ,  $SO_4^{2-}$ ,  $Cl^-$ , and  $HCO_3^-$  in a water sample. Corresponding analysis could be conducted according to the distributions of the six ions. The Piper trilinear diagram could illustrate the hydrochemical characteristics of groundwater through the relative compositions of the chemical components [25].

The Piper trilinear diagram was plotted based on the data of 47 water samples (Figure 4). As shown in Figure 4, the result demonstrated all water samples belong to  $NaSO_4$ -type water, and the cationic compositions of the three water source types were quite different. Sample 10 (from the Ordovician limestone aquifer) and sample 45 (from the Shanxi Formation sandstone aquifer) have notably different hydrochemical characteristics, as marked by the red oval area.

The cluster analysis refers to the analysis process of grouping a set of physical or abstract objects into multiple classes composed of similar objects [26]. It classified the research objects (samples or indexes) according to their characteristics to exclude abnormal objects. Specifically, each

water sample is regarded as a vector comprising  $n$  indexes, and the space composed of  $n$ -dimensional vectors is approximated as the distance space [27]. Under the condition that other factors exert a limited effect, the groundwater samples from the same source or with the same hydrochemical characteristics could be classified into one category because of the relatively short distance between them, while those from different sources or with different hydrochemical characteristics could be classified into different categories.

In this paper, the cluster analysis was also conducted based on the data of 47 water samples (Figure 5). The cluster analysis results also reveal the distinct hydrochemical characteristics of samples 10 and 45 from the Piper diagram as those of other samples. This confirms that the two exceptional samples should be excluded from further analysis.

#### Step 3. Establishment of an index system.

With the contents of six ions  $Na^+ + K^+$ ,  $Ca^{2+}$ ,  $Mg^{2+}$ ,  $SO_4^{2-}$ ,  $Cl^-$ , and  $HCO_3^-$  in the water samples taken as the indexes, the index set named as  $U = \{Na^+ + K^+, Ca^{2+}, Mg^{2+}, SO_4^{2-}, Cl^-, HCO_3^-\}$  is established.

The evaluation set of water source types for the identification model, i.e.,  $V = \{\text{Shanxi Formation sandstone water, Taiyuan Formation limestone water, and Ordovician limestone water}\}$ , was established in accordance with the three water sources types (represented by I, II, and III, respectively).

#### Step 4. Weight assignments for the indexes.

The objective weights of the indexes were calculated based on the mass concentration data of six indexes  $Na^+ + K^+$ ,  $Ca^{2+}$ ,

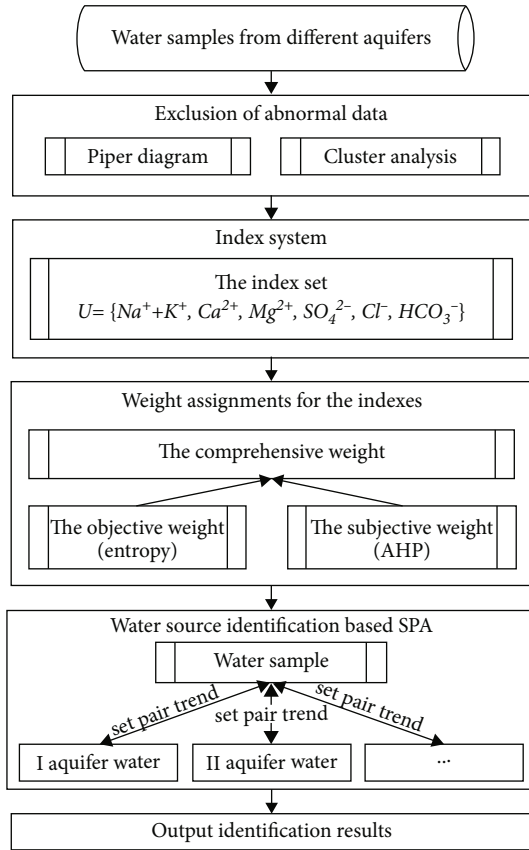


FIGURE 3: Workflow of identification of groundwater source.

$Mg^{2+}$ ,  $SO_4^{2-}$ ,  $Cl^-$ , and  $HCO_3^-$  of the remaining 45 water samples (abnormal samples excluded). Next, the subjective weights and the comprehensive weights of the indexes were calculated through Equations (4) and (5) in the AHP-entropy weight method. The calculation results are listed in Table 1.

Step 5. Groundwater source identification based on SPA.

The box plot reflecting the mass concentration variations of various ions in different aquifers was drawn based on the remaining 45 water samples (Figure 6). The box plot is a statistical method that reflects the distribution characteristics of the original data [28]. The standard of response data characteristics of the box plot is based on the quartiles and the interquartile range. The quartiles have certain resistance. Up to 25% of the data could become arbitrarily far away without greatly disturbing the quartile. Using the upper and lower quartiles of the box plot as the water source discrimination interval could objectively reflect the hydrochemical characteristics of aquifers [29]. The upper quartile and lower quartile of the box plot are set as the lower limit  $S_2$  and upper limit  $S_3$  of a certain index in the water source type's membership interval, and then, the corresponding  $S_1$  and  $S_4$  were calculated through Equation (8). The results are given in Table 2.

Then, the components of connection degree and the set pair trends between each water sample and each water source type's identification interval could be calculated through Equations (9) and (10) in the SPA theory we men-

tioned above. The water source to which the sample belongs is determined by comparing the set pair trends.

4.2. Model Validation and Analysis. The established identification model was utilized to identify another 10 samples ( $W_1$  to  $W_{10}$ ) taken from Chengjiao coal mine for verifying its accuracy. The samples to be identified and the identification results are exhibited in Table 3. Shanxi Formation sandstone water, Taiyuan Formation limestone water, and Ordovician limestone water were represented by I, II, and III, respectively.

A comparison between the identification results and the actual water source types indicates that for all the 10 samples, the identification results and the actual situation were completely consistent, which means the model achieves 100% identification accuracy. However, the values of  $t_I$  and  $t_{II}$  in the set pair trends of water sample  $W_1$  were very close, which will reduce the confidence of the final identification result. There are two possible reasons for this phenomenon: One is the water sample  $W_1$  may come from mixed water of more than one aquifer, which leads to an increase in the connection degree between some indexes of multiple aquifers in the SPA-based identification model, then resulting in the similar set pair trends calculated. On the other hand, the model employs too few water samples in each aquifer as the basis to fully reflect the hydrochemical characteristics of the aquifer, therefore increasing the error of the identification results. Additionally, FDA and BDA were also employed for groundwater source identification and their identification accuracy rates were 70% and 80%, respectively. To sum up, the SPA-based identification model performed better in identifying the sources of water samples.

4.3. Determination of the Source of Water Inflow in No. 21304 Working Face. A water sample collected from the No. 21304 panel was identified by using the model established above. The sample and identification result are disclosed in Table 4.

According to the identification result, there is no doubt that the Ordovician limestone aquifer water was the major source of inflow of the No. 21304 panel and that the Taiyuan Formation limestone aquifer water may be highly related to the inflow water. However, there is only a minuscule chance that the Shanxi Formation sandstone aquifer water relates to the inflow.

It is assumed that the three aquifers all contribute to water inflow in the No. 21304 panel to further verify the accuracy of the above identification results in this paper. According to the principle that the content of each ion component of the mixed solution is constant, the element composition and content remain unchanged after the water of the three water source types is mixed to form mine water. The migration of groundwater is accompanied by ion exchange, which will lead to the alternating adsorption of  $Na^+ + K^+$  and  $Ca^{2+} + Mg^{2+}$  by rocks, resulting in the change in the concentration of  $Na^+$ ,  $K^+$ ,  $Ca^{2+}$ , and  $Mg^{2+}$  in water [30]. Meanwhile, the content of  $HCO_3^-$  in water is also easily affected by other ions and pH. However,  $SO_4^{2-}$  and  $Cl^-$  whose contents are less affected by other ions and pH will not be

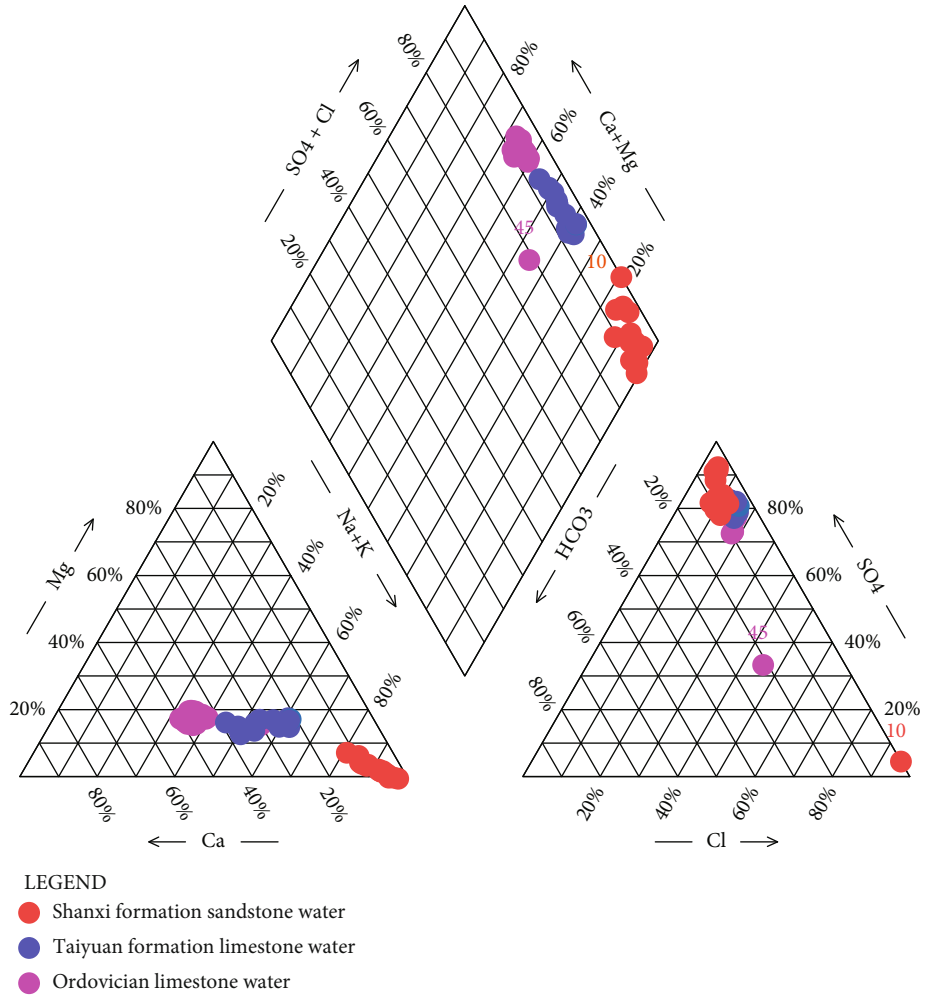


FIGURE 4: Piper diagram of water samples from different aquifers.

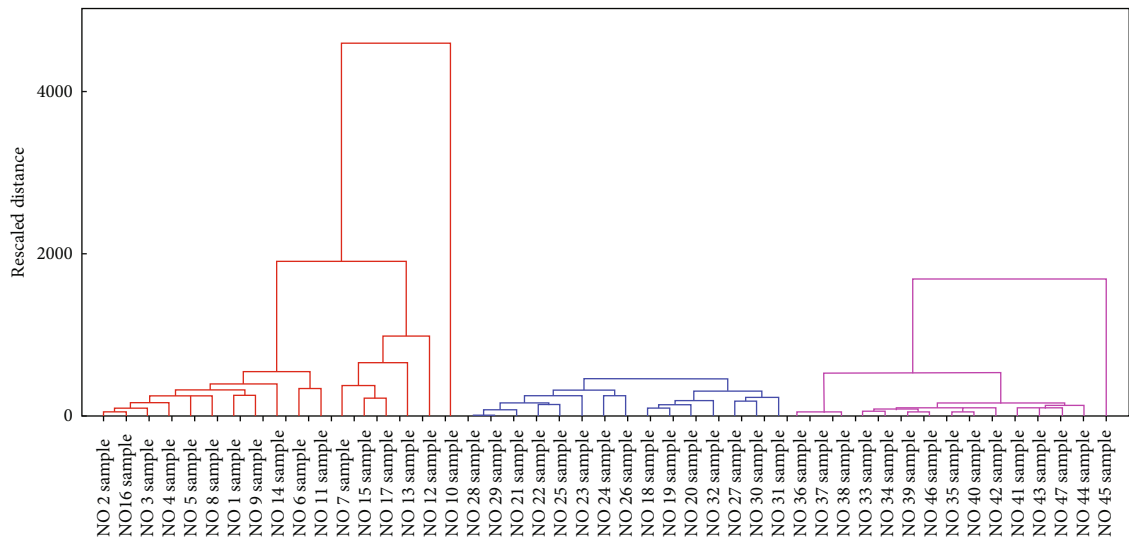


FIGURE 5: Cluster analysis of water samples (red: Shanxi Formation sandstone aquifer; blue: Taiyuan Formation limestone aquifer; pink: Ordovician limestone aquifer).

TABLE 1: Weights of the indexes.

Weights	$K^+Na^+$	$Ca^{2+}$	$Mg^{2+}$	$SO_4^{2-}$	$Cl^-$	$HCO_3^-$
Objective weights	0.27	0.31	0.23	0.07	0.05	0.07
Subjective weights	0.17	0.16	0.18	0.22	0.17	0.10
Comprehensive weights	0.27	0.29	0.25	0.09	0.06	0.04

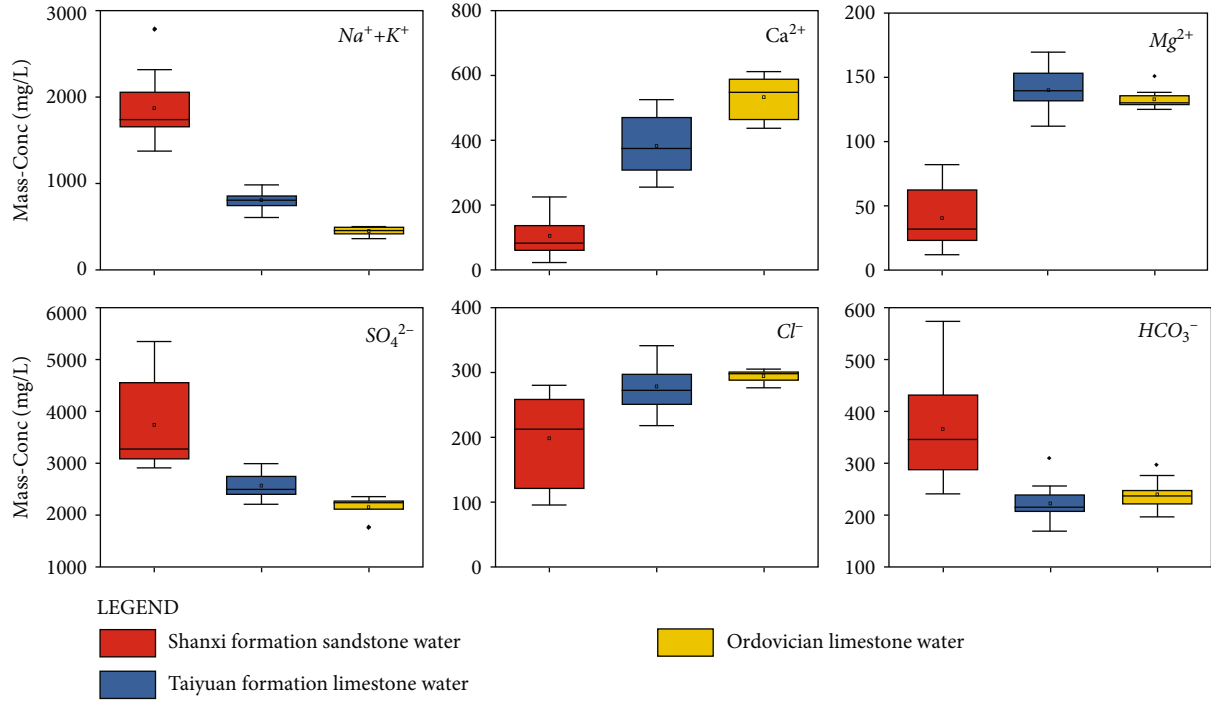


FIGURE 6: Box plot of six indexes.

TABLE 2: Limits of six indexes.

Water source type	Index	$S_1$	$S_2$	$S_3$	$S_4$
Shanxi Formation sandstone aquifer	$K^+Na^+$	1479.68	1662.08	2026.88	2209.28
	$Ca^{2+}$	24.83	62.29	137.21	174.66
	$Mg^{2+}$	5.74	23.04	57.65	74.95
	$SO_4^{2-}$	2439.16	3092.57	4399.39	5052.79
	$Cl^-$	61.15	125.85	255.25	319.95
	$HCO_3^-$	220.27	289.45	427.81	497.00
Taiyuan Formation limestone aquifer	$K^+Na^+$	706.51	756.47	856.37	906.32
	$Ca^{2+}$	231.38	309.55	465.90	544.07
	$Mg^{2+}$	123.43	131.67	148.16	156.40
	$SO_4^{2-}$	2280.57	2427.19	2720.43	2867.05
	$Cl^-$	238.30	257.90	297.11	316.71
	$HCO_3^-$	196.68	209.94	236.46	249.72
Ordovician limestone aquifer	$K^+Na^+$	392.21	427.21	497.22	532.22
	$Ca^{2+}$	413.88	471.30	586.15	643.58
	$Mg^{2+}$	124.78	128.27	135.25	138.74
	$SO_4^{2-}$	2066.11	2134.70	2271.86	2340.44
	$Cl^-$	286.12	290.69	299.84	304.41
	$HCO_3^-$	210.88	222.50	245.73	257.34

TABLE 3: Samples to be identified and identification results.

Sample	Sample data (unit: mg/L)						Set pair trend			SPA	FDA	BDA	Actual
	$K^+Na^+$	$Ca^{2+}$	$Mg^{2+}$	$SO_4^{2-}$	$Cl^-$	$HCO_3^-$	$t_I$	$t_{II}$	$t_{III}$				
$W_1$	1534.83	267.14	92.77	2465.36	255.39	248.86	2.77	2.08	0.67	I	I	II	I
$W_2$	1347.93	225.41	83.18	3155.16	274.12	307.89	3.06	1.34	0.47	I	I	I	I
$W_3$	1357.54	237.65	121.67	3311.33	129.75	266.59	2.37	1.33	0.79	I	I	II	I
$W_4$	706.30	360.78	120.02	2247.41	273.34	232.90	1.18	6.78	1.87	II	II	II	II
$W_5$	721.84	263.88	113.11	2047.28	274.74	235.00	1.38	4.29	1.15	II	II	II	II
$W_6$	780.75	202.24	109.31	1977.25	243.05	170.69	1.72	3.58	0.75	II	II	II	II
$W_7$	865.56	342.14	112.99	2572.35	276.51	200.18	1.32	9.90	0.99	II	II	II	II
$W_8$	484.00	463.51	118.59	2018.03	285.37	164.10	0.97	3.15	5.75	III	II	III	III
$W_9$	510.40	579.82	134.19	2316.10	297.78	257.41	0.94	3.57	23.19	III	II	III	III
$W_{10}$	565.56	493.56	127.58	2272.08	286.93	269.62	1.03	4.14	8.27	III	II	III	III

TABLE 4: Samples of No. 21304 working face and identification results.

Sample of No. 21304 working face (unit: mg/L)						Set pair trend		
$K^+Na^+$	$Ca^{2+}$	$Mg^{2+}$	$SO_4^{2-}$	$Cl^-$	$HCO_3^-$	$t_I$	$t_{II}$	$t_{III}$
542.00	524.31	143.42	2217.55	296.72	206.74	0.89	4.57	5.73

adsorbed in rock mass and soil, so they are relatively stable ions in groundwater. Based on this premise, the mass balance equation of  $SO_4^{2-}$  and  $Cl^-$  could be established to calculate the relative proportion of the sources of water inflow.

$$\begin{bmatrix} 369.1 & 278.1 & 305.6 \\ 3537.7 & 2560.6 & 2037.3 \\ 1 & 1 & 1 \end{bmatrix} \begin{bmatrix} m_I \\ m_{II} \\ m_{III} \end{bmatrix} = \begin{bmatrix} 296.7 \\ 2217.6 \\ 1 \end{bmatrix}, \quad (11)$$

where  $m_I$ ,  $m_{II}$ , and  $m_{III}$  are the proportions of the Shanxi Formation sandstone aquifer water, the Taiyuan Formation limestone aquifer water, and the Ordovician limestone aquifer water of total panel inflow, respectively.

Solving Equation (11) yields  $m_I = 0.0042$ ,  $m_{II} = 0.3325$ , and  $m_{III} = 0.6633$ . The results show that the Ordovician limestone aquifer water accounts for 66.33% of total water inflow, while the Taiyuan Formation limestone aquifer and the Shanxi Formation sandstone aquifer water account for 33.25% and 0.42% of water inflow, respectively. This is basically consistent with the results of the groundwater source identification model based on the AHP-entropy weight method and the SPA theory, so the results of the model are reliable.

Specific water inrush controlling measures should be formulated for the three aquifers due to their varying water abundances. Although the Shanxi Formation sandstone aquifer is the closest to the  $II_2$  coal seam, its maximum unit water inflow is only 0.07 L/s-m. Considering its poor water abundance, its threat of water disaster could generally be

eliminated through measures such as temporary water bin construction in low-lying areas and water pump installation. In contrast, the Taiyuan Formation and the Ordovician limestone aquifer possess abundant water, with their maximum unit water inflows being 2.87 L/s-m and 3.56 L/s-m, respectively. As a result, their water disasters are often controlled by measures such as aquiclude grouting reinforcement and water-resisting coal pillar retention.

Accordingly, the Ordovician limestone aquifer water was the major source of inflow of the No. 21304 panel. In the follow-up production, the area of the No. 21304 panel that is close to the  $F_{20}$  fault should be regarded as the focus of attention. In this area, safer and stricter mining methods, as well as more reliable and effective prevention and control measures, such as aquiclude reinforcement by grouting and water-resisting coal pillar retention, should be adopted to ensure production safety in the panel.

## 5. Conclusions

The identification of mine groundwater source is a complex problem. Under the influences of multiple factors, it is difficult to identify the groundwater sources accurately in the coal mining processing. Quick and accurate identification of mine groundwater source is of great significance to the prevention and control of water inrush accidents in coal mines. Thus, a reliable method is urgently needed to solve this problem.

In this study, the hydrochemical characteristics of water sources from different aquifers in Chengjiao coal mine were determined by means of the Piper trilinear diagram and the cluster analysis, and ions in the groundwater were analyzed



by combining the AHP-entropy weight method and the SPA theory. On the basis of the analysis results, a mine groundwater source identification model was established, and the identification reliability of the model was verified. The verification results were showed that the model based on the AHP-entropy weight method and the SPA theory performs better in identifying the groundwater source compared with those established using FDA and BDA methods.

After systematical analysis of the established model, the source of water inflow in the No. 21304 panel was identified, and the primary source was revealed. The analysis on the identification results reveals that the area close to the  $F_{20}$  fault tends to receive water supply from the Ordovician limestone aquifer and the Taiyuan Formation limestone aquifer, so it should be regarded as the key area for mine water inrush prevention and control.

### Data Availability

The data used to support the findings of this study are included within the article.

### Conflicts of Interest

The authors declare no conflict of interest.

### Acknowledgments

This work was supported by the Chengjiao Coal Mine in Henan Province, China. This research was financially supported by the National Key Research and Development Program of China (No. 2019YFC1805400), the National Nature Science Foundation of China (42172272), the Fundamental Research Funds for the Central Universities (No. 2020ZDPY0201), and the National Science Foundation of China (No. U1710253).

### Supplementary Materials

The tables of 47 water samples from different aquifers (Line 187), classification function coefficients of the FDA method (Line 272), and classification function coefficients of the BDA method (Line 272) are in the supplementary files. (*Supplementary Materials*)

### References

- [1] P. Bukowski, "Water hazard assessment in active shafts in upper Silesian coal basin mines," *Environment*, vol. 30, no. 4, pp. 302–311, 2011.
- [2] B. Luo, Y. Sun, Z. Xu et al., "Damage characteristics and mechanism of the 2017 groundwater inrush accident that occurred at Dongyu coalmine in Taiyuan," *Water*, vol. 13, no. 3, p. 2021, 2021.
- [3] H. Yin, C. Zhao, Y. Zhai et al., "Application of comprehensive support techniques to roadway tunneling in vicinity of Ordovician carbonate confined aquifers under complicated tectonic conditions," *Carbonates and Evaporites*, vol. 35, no. 4, 2020.
- [4] D. Dong, Z. Chen, G. Lin, X. Li, R. Zhang, and Y. Ji, "Combining the fisher feature extraction and support vector machine methods to identify the water inrush source: a case study of the Wuhai mining area," *mine water and the Environment*, vol. 38, no. 4, pp. 855–862, 2019.
- [5] G. Vizintin, M. Veselic, A. Bombac, E. Dervaric, J. Likar, and Z. Vukelic, "The development of a "drive-in" filters dewatering system in the Velenje coal mine using finite-element modeling," *Acta Geotechnica Slovenica*, vol. 6, no. 1, pp. 50–63, 2009.
- [6] F. Hu, M. Zhou, P. Yan et al., "Selection of characteristic wavelengths using SPA for laser induced fluorescence spectroscopy of mine water inrush," *Spectrochimica Acta Part A: Molecular and Biomolecular*, vol. 219, pp. 367–374, 2019.
- [7] Y. B. Du, Y. S. Zheng, G. Wu, and Y. Tang, "Decision-making method of heavy-duty machine tool remanufacturing based on AHP-entropy weight and extension theory," *Journal of Cleaner Production*, vol. 252, 2020.
- [8] M. Peters and S. Zelewski, "Pitfalls in the application of analytic hierarchy process to performance measurement," *Management Decision*, vol. 46, no. 7, pp. 1039–1051, 2008.
- [9] G. D. Wu, K. F. Duan, J. Zuo, X. B. Zhao, and D. Z. Tang, "Integrated sustainability assessment of public rental housing community based on a hybrid method of AHP-entropy weight and cloud model," *Sustainability*, vol. 9, 2017.
- [10] Z. An and L. R. Song, "Research on the role of AHP- entropy method in the identification and evaluation of China tariff source risk," *Journal of Intelligent & Fuzzy Systems*, vol. 34, no. 2, pp. 1053–1060, 2018.
- [11] Z. K. Ding, M. L. Zhu, Z. Z. Wu, Y. B. Fu, and X. Liu, "Combining AHP-entropy approach with GIS for construction waste landfill selection-a case study of Shenzhen," *International journal of environmental research and public health*, vol. 15, no. 10, 2018.
- [12] G. Z. Feng, S. Y. Lei, Y. J. Guo, B. Meng, and Q. F. Jiang, "Optimization and evaluation of ventilation mode in marine data center based on AHP-entropy weight," *Entropy*, vol. 21, no. 8, 2019.
- [13] Y. Cao, Y. Cao, H. Zhou, H. Zhou, J. Wang, and J. Wang, "An approach to interval-valued intuitionistic stochastic multicriteria decision-making using set pair analysis," *International Journal of Machine Learning and Cybernetics*, vol. 9, no. 4, pp. 629–640, 2018.
- [14] C. Wei, X. Dai, S. Ye, Z. Guo, and J. Wu, "Prediction analysis model of integrated carrying capacity using set pair analysis," *Ocean & Coastal Management*, vol. 120, pp. 39–48, 2016.
- [15] Y. Liu, "Assessment of building sustainable performance based on set pair analysis (SPA)," *Materials Research*, vol. 255–260, pp. 94–98, 2011.
- [16] T. Chong, S. Yi, and C. Heng, "Application of set pair analysis method on occupational hazard of coal mining," *SAFETY SCIENCE*, vol. 92, pp. 10–16, 2017.
- [17] Q. Wei and Z. J. Zhao, "Research on evaluation of coastal city water sports tourism resources based on set pair analysis," *Journal of Coastal Research*, vol. 115, pp. 190–192, 2020.
- [18] M. R. Su, Z. F. Yang, and B. Chen, "Set pair analysis for urban ecosystem health assessment," *Communications in Nonlinear Science and Numerical Simulation*, vol. 14, no. 4, pp. 1773–1780, 2009.
- [19] K. Kumar, K. Kumar, H. Garg, and H. Garg, "Connection number of set pair analysis based TOPSIS method on intuitionistic fuzzy sets and their application to decision making," *Applied Intelligence*, vol. 48, no. 8, pp. 2112–2119, 2018.
- [20] Y. C. Liu, C. S. Wang, Y. T. Chun, L. X. Yang, W. Chen, and J. Ding, "A novel method in surface water quality assessment

- based on improved variable fuzzy set pair analysis,” *International Journal of Environmental Research and Public Health*, vol. 16, no. 22, 2019.
- [21] J. Zhang, Y. Li, C. Liu et al., “Application of set pair analysis in a comprehensive evaluation of water resource assets: a case study of Wuhan City, China,” *Water*, vol. 11, no. 8, 2019.
- [22] F. S. Yang, C. J. Xu, X. M. Huang, and J. R. Shao, “Improved set pair analysis model for urban water security assessment,” *Advanced Materials Research*, vol. 1065, pp. 2903–2908, 2015.
- [23] G. He, K. Bao, W. Wang, Y. Zhu, S. Li, and L. Jin, “Assessment of ecological vulnerability of resource-based cities based on entropy-set pair analysis,” *Environmental Technology*, vol. 42, pp. 1–11, 2021.
- [24] P. Li, Y. Zhang, N. Yang, L. Jing, and P. Yu, “Major ion chemistry and quality assessment of groundwater in and around a mountainous tourist town of China,” *Exposure and Health*, vol. 8, no. 2, pp. 239–252, 2016.
- [25] N. Subba Rao, B. Ravindra, and J. Wu, “Geochemical and health risk evaluation of fluoride rich groundwater in Sattenapalle region, Guntur district, Andhra Pradesh, India,” *Human and ecological risk assessment: An international journal*, vol. 26, no. 9, pp. 2316–2348, 2020.
- [26] N. Subba Rao, A. Dinakar, B. K. Kumari, D. Karunanidhi, and T. Kamalesh, “Seasonal and spatial variation of groundwater quality vulnerable zones of Yellareddygudem watershed, Nalgonda District, Telangana State, India,” *Archives of environmental contamination and toxicology*, vol. 80, no. 1, pp. 11–30, 2021.
- [27] Y. Chen, S. Zhu, and S. Xiao, “Discussion on controlling factors of hydrogeochemistry and hydraulic connections of groundwater in different mining districts,” *Natural Hazards*, vol. 99, no. 2, pp. 689–704, 2019.
- [28] N. S. Rao, A. Dinakar, M. Sravanthi, and B. K. Kumari, “Geochemical characteristics and quality of groundwater evaluation for drinking, irrigation, and industrial purposes from a part of hard rock aquifer of South India,” *Environmental Science and Pollution Research*, vol. 28, no. 24, pp. 31941–31961, 2021.
- [29] J. Zhang and D. Yao, “Hydrogeochemical characteristics of coal mine based on box-plot and its application in water inrush source identification,” *Part A, Recovery, utilization, and environmental effects*, pp. 1–14, 2020.
- [30] H. Zhang, G. Xu, X. Chen, and A. Mabaire, “Hydrogeochemical evolution of multilayer aquifers in a massive coalfield,” *Environmental Earth Sciences*, vol. 78, no. 24, 2019.